Synthesis, chemical characterisation and spectroscopic studies of the six-coordinate 3-halo-2,6-lutidine *N*-oxide complex [PrCl$_3$(H$_2$O)(BrC$_7$H$_8$NO)$_2$]H$_2$O — a new Pr(III) compound

L. Macalik[a,*], J. Hanuza[a], K. Hermanowicz[a], W. Oganowski[a], H. Ban-Oganowska[b]

[a]*W. Trzebiatowski Institute for Low Temperature and Structure Research, Polish Academy of Sciences, P.O. Box 937, 50-950 Wrocław 2, Poland*
[b]*Department of Organic Chemistry, Academy of Economics, 53-345 Wrocław, Poland*

Abstract

New compounds derived from 3-halo-2,6-lutidine *N*-oxides were synthesized as potential precursors to light-conversion molecular materials. The synthesis, chemical characterisation and spectroscopic studies of the six-coordinate praseodymium(III) complex with the bromide derivative are reported. IR and Raman spectra were measured and are discussed in terms of the possible structure and composition of this compound. The electronic absorption, emission and excitation spectra were recorded and analysed. The $^3P_0 \rightarrow {}^3H_{4,5,6}$ emissions were observed. Selective excitation in the UV region was used to assign the energy levels of Pr^{3+} in this complex.   © 2000 Elsevier Science S.A. All rights reserved.

Keywords: Pr(III) complexes; 3-Halo-2,6-lutidine *N*-oxides; Light-conversion molecular devices

1. Introduction

Pyridine *N*-oxide complexes of transition elements have been studied in detail by several authors. These studies are reviewed by Garvey et al. [1], Carlin and De Jongh [2] and Quagliano et al. [3–5]. However, the lanthanide complexes with these ligands are still not well documented. Except for picoline *N*-oxide complexes of europium chloride, perchlorate and hexafluorophosphate [6], and some pyridine *N*-oxide complexes with light lanthanides of the Ln:ligand=1:8 type [7], no other compounds, to our knowledge, have been reported in the literature. The crystal structures of two complexes of this type, Ln(PyO)$_8$(ClO$_4$)$_3$, for lanthanum and neodymium have been studied by Razzak et al. [8].

Our studies are concerned with the synthesis of the new praseodymium(III) complex derived from 3-bromo-2,6-lutidine *N*-oxide (BLNO) with composition Pr:ligand=1:2. This compound was characterised by means of different spectroscopic methods: IR, Raman, electronic absorption, emission and excitation spectra. Materials such as this could be used in possible light-conversion molecular

devices. The complex studied is an example of the wide class of six-coordinate Ln(III) compounds with HLNO ligands.

2. Experimental

2.1. Synthesis

Praseodymium(III) oxide (0.173 g) (99.99%) was dissolved in 4 ml of an aqueous solution of hydrochloric acid (1 N) at 90°C. The solution obtained was evaporated at 95–105°C giving the powdered praseodymium chloride hydrate, which was then dissolved in 10 ml of 99.8% ethanol. 3-Bromo-2,6-lutidine *N*-oxide (0.606 g) was added to this solution and briefly stirred giving a clear solution. This mixture of the salt and the ligand remains unchanged for a long time when stored at ambient temperature (even after a few days). However, irradiation with a quartz lamp for 4 min gives (after 15 min) a green-yellow crystalline product. The mixture of the solution and the residue was subsequently stored at 4°C for 24 h, filtered, washed three times with ethanol and dried in vacuum over silica-gel. The composition of the complex was established by microanalysis giving the stoichiometry:

*Corresponding author.
E-mail address: lmacalik@highscreen.int.pan.wroc.pl (L. Macalik)

[PrCl$_3$(H$_2$O)(BrC$_7$H$_8$NO)$_2$]H$_2$O; calc.: C 24.443, H 2.932, N 4.075 and Pr 20.499 wt%; found: C 24.829, H 3.136 and N 3.460, molecular weight 687.381 g. The total yield of the complex was 75%.

The purity of the obtained complex was verified by chemical, spectroscopic and XRD methods. No uncontrollable doping (detectable by these techniques) exists in the samples studied. The 15% discrepancy between the calculated and experimental nitrogen content is caused by the low accuracy of the methods used in the determination of the amount of this element.

2.2. Spectral measurements

IR spectra in the range 10–4000 cm^{-1} were recorded in Nujol suspensions and a KBr tablet with a FTIR Biorad 575C spectrometer. The resolution was 0.5 cm^{-1} in the MIR range and 1 cm^{-1} in the FIR range. Raman spectra were measured in 90° scattering geometry with a Nicolet Magna-IR 860 spectrometer. The resolution was 1 cm^{-1}. Electronic absorption spectra were recorded in the region 200–3700 nm with a Cary 5E spectrophotometer. The emission and excitation spectra were recorded on a SSF

spectrofluorometer using an argon ion laser ILA 120 and a xenon lamp.

3. Results

3.1. IR and Raman spectra

The IR and Raman spectra of the ligand and its praseodymium complex are shown in Fig. 1. The observed bands are listed in Table 1 together with the assignment of the respective vibrational modes. The description of the bands is based on our previous work concerning the vibrational behaviour of pyridine N-oxides [9–12].

The IR and Raman spectra of the free ligand exhibit the typical pattern expected for pyridine N-oxide ring vibrations coupled with two CH$_3$ groups' modes. The ν(N–O), δ(N–O) and γ(N–O) modes occur at about 1267 (IR), 540 (RS) and 310 (RS). The carbon–bromide vibrations are also easily attributable to the bands at 330 cm^{-1} ν(C–Br) and 280 cm^{-1} δ(C–Br). In the spectra of the praseodymium complex all these bands remain virtually unchanged. The ν(N–O) modes shift in the IR spectrum to 1223 cm^{-1}. The ν(N–O) Raman line shifts from 1229

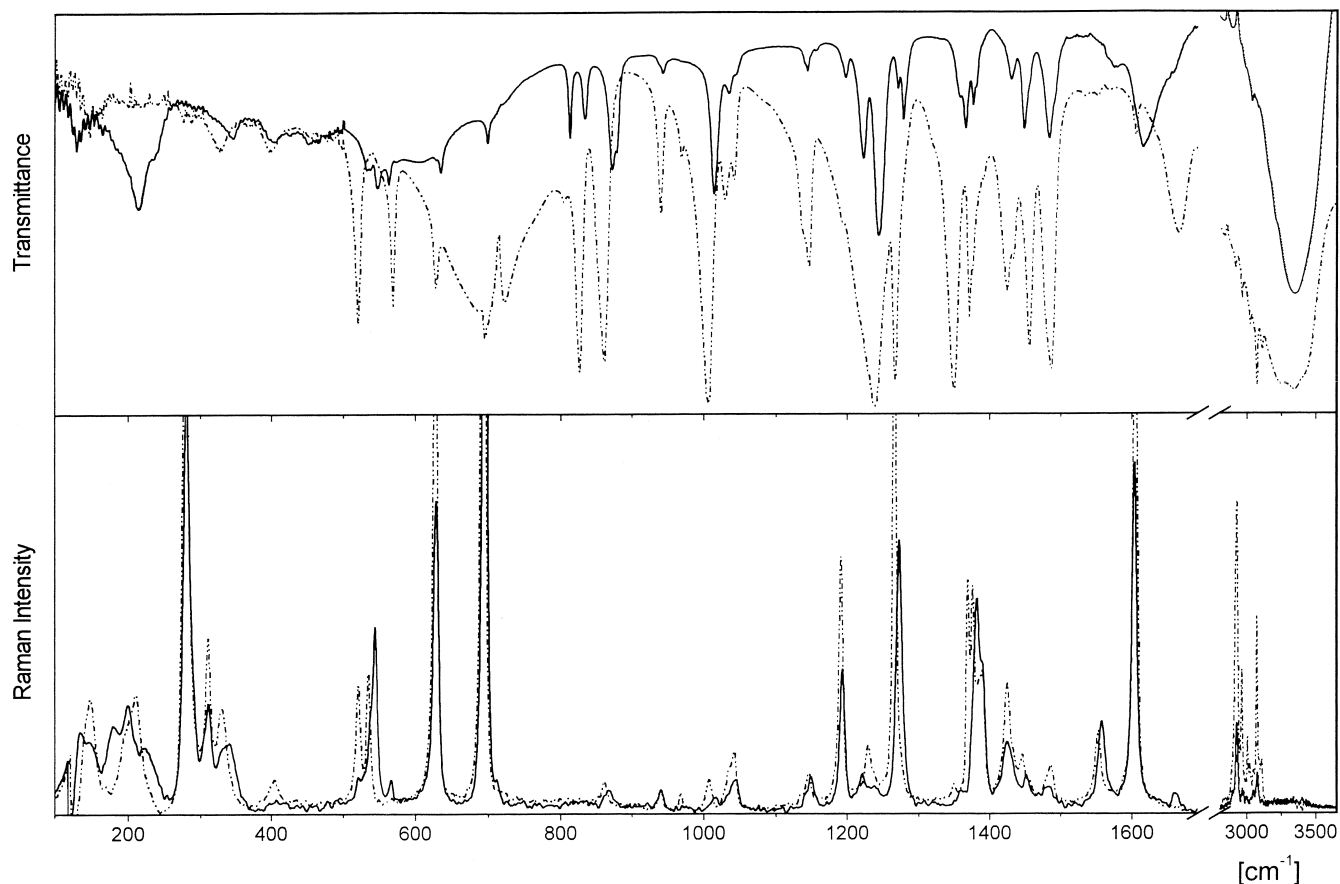Fig. 1. IR and Raman spectra of the ligand and its praseodymium complex measured at room temperature [(———) PrCl$_3$(H$_2$O)L$_2$ and (– · –) L=(BrC$_7$H$_8$NO)].

Table 1
Raman and IR spectra of the ligand and the [PrCl$_3$(H$_2$O)(BrC$_7$H$_8$NO)$_2$]H$_2$O complex and the band assignment to the respective vibrational modes (vs, very strong; s, strong; m, middle; w, weak; vw, very weak; b, broad; sh, shoulder)

Raman (cm^{-1})		IR (cm^{-1})		Assignment
Ligand	Complex	Ligand	Complex	
	134 w		128 w	δ(O–Pr–O)
147 m	146 m	147 vw		ligand skeletal vibration
169 sh				γ(C–Br) and ν(Pr–O)
193 m	178 m		182 sh	
203 sh	200 m		213 w	
210 m	223 m		235 sh	
279 vs	280 s	284 w		δ(O–Br)
310 m	310 m			γ(N–O)
330 m	340 m	332 w	345 w	ν(C–Br)
403 w	406 sh	400 w	404 w, 451 w	ν$_{16a}$
520 m	520 w	520 m	530 w	ν$_{16b}$
533 m	542 m		546 w	δ(N–O)
548 sh				
	565 w	568 m	561 w	ν$_{6a}$
628 s	629 s	628 m	635 m	ν$_{6b}$
693 vs	694 vs	695 m	698 w	ν$_4$
	711 sh			
			812 m	δ(N–O)
		803 sh		ν$_1$
		826 m	832 m	
			840 sh	
860 vw	866 vw	860 m	871 m	γ(CH)
	879 vw		878 sh	
	921 vw			ν(C–CH$_3$)
939 vw	940 vw	940 w	942 w	
968 vw		968 sh	968 sh	ρ(CH$_3$)
1007 w	1016 w	1006 s	1014 m	ν$_{12}$
		1029 w	1034 w	ρ(CH$_3$)
1042 w	1044 m	1043 w	1045 sh	
		1084 w	1072 vw	
1133 sh				δ(CH)
1145 w	1147 w	1146 w	1143 w	
1191 s	1193 m		1197 sh	
1229 m	1221 w	1267 m	1223 m	ν(N–O)
	1237 vw	1238 s	1242 m	δ(CH)
1266 vs	1272 s		1270 w	ω in plane ring def.+
			1280 w	ν(N–O)
1349 sh	1359 sh	1350 m	1358 sh	ν$_s$(CH$_3$)
1369 s		1372 m	1360 w	
1376 s		1376 sh	1376 w	
1389 m	1382 s			
1424 m	1423 m	1424 w	1429 w	δ$_{as}$(CH$_3$)
1445 w	1450 w	1456 m	1448 m	ν$_{19b}$ ring stretch
1479 sh				
1485 w	1482 w	1486 m	1482 m	ν$_{19a}$ ring stretch
1552 m	1557 m		1574 sh	δ(HOH) and ν$_{8a}$ and ν$_{8b}$
1589 sh		1606 vw	1615 m	ring stretch
1605 vs	1603 s	1664 w		
	1657 vw	1694 sh	1655 sh	
2888 sh	2897 sh			ν$_s$(CH$_3$)
2926 s	2926 m			
2964 m	2967 w			ν$_{as}$(CH$_3$)
2989 sh	2997 w			
3005 w				ν(CH)
3019 w	3025 w	3020 w		
3046 w	3043 w			
3072 m	3074 w	3072 m		
3085 sh				
3107 w	3104 vw	3108 w		
		3236 m,b	3320 w	ν(OH)
3256 vw,b	3333 vw	3276 sh	3440 w,b	
		3340 m,b	3568 w	

cm^{-1} in the free ligand spectrum to 1221 cm^{-1} in the spectrum of the complex. The significant shift of the IR line (44 cm^{-1}) in comparison with the Raman line (8 cm^{-1}) demonstrates that the dipole interactions play an important role in the complexation of this ligand and the polarizability changes are quite small. The strong intensity

bands of the ligand observed at 826, 860 and 1006 cm^{-1} shift for the praseodymium complex to higher frequencies, 832, 871 and 1014 cm^{-1}, respectively. They correspond to the γ(CH) and ring breathing vibrations. The new IR band observed at 812 cm^{-1} is probably due to the δ(N–O) bending vibration. The two new bands observed at 220 and

130 cm^{-1} can be assigned to stretching ν(Pr–O) and bending δ(O–Pr–O) vibrations. They are broad and display medium intensity having several distinct components.

The vibrational spectra clearly suggest coordination through the oxygen atom because the involvement of the metal ion in the coordination moiety causes a decrease of the bond order in the N=O group, owing to donation of electron density to the metal ion.

The complex exhibits broad bands centered at about 3400 and 1630 cm^{-1} due to the stretching and bending modes of coordinated and lattice water. In addition, weak bands are detectable in the 800–850 cm^{-1} region which could be assigned to the rocking modes of a water molecule coordinated to the praseodymium ion. The

presence of water bound in two different ways is confirmed by the results of thermogravimetric analysis.

3.2. Electronic absorption spectra

The room temperature electronic absorption spectrum of the complex is presented in Fig. 2. Several bands are observed in the visible and NIR region. The lines appearing in the visible region correspond to transitions from the $^3H_4$ ground state to $^3P_2$ (22,523 cm^{-1}), $^1I_6 + {}^3P_1$ (21,368 cm^{-1}), $^3P_0$ (20,747 cm^{-1}) and $^1D_2$ (16,978, 16,750 cm^{-1}). The transitions $^3H_4 \rightarrow {}^1G_4$ at 9823 and 9606 cm^{-1} are also detected, although their intensities are quite weak. In the

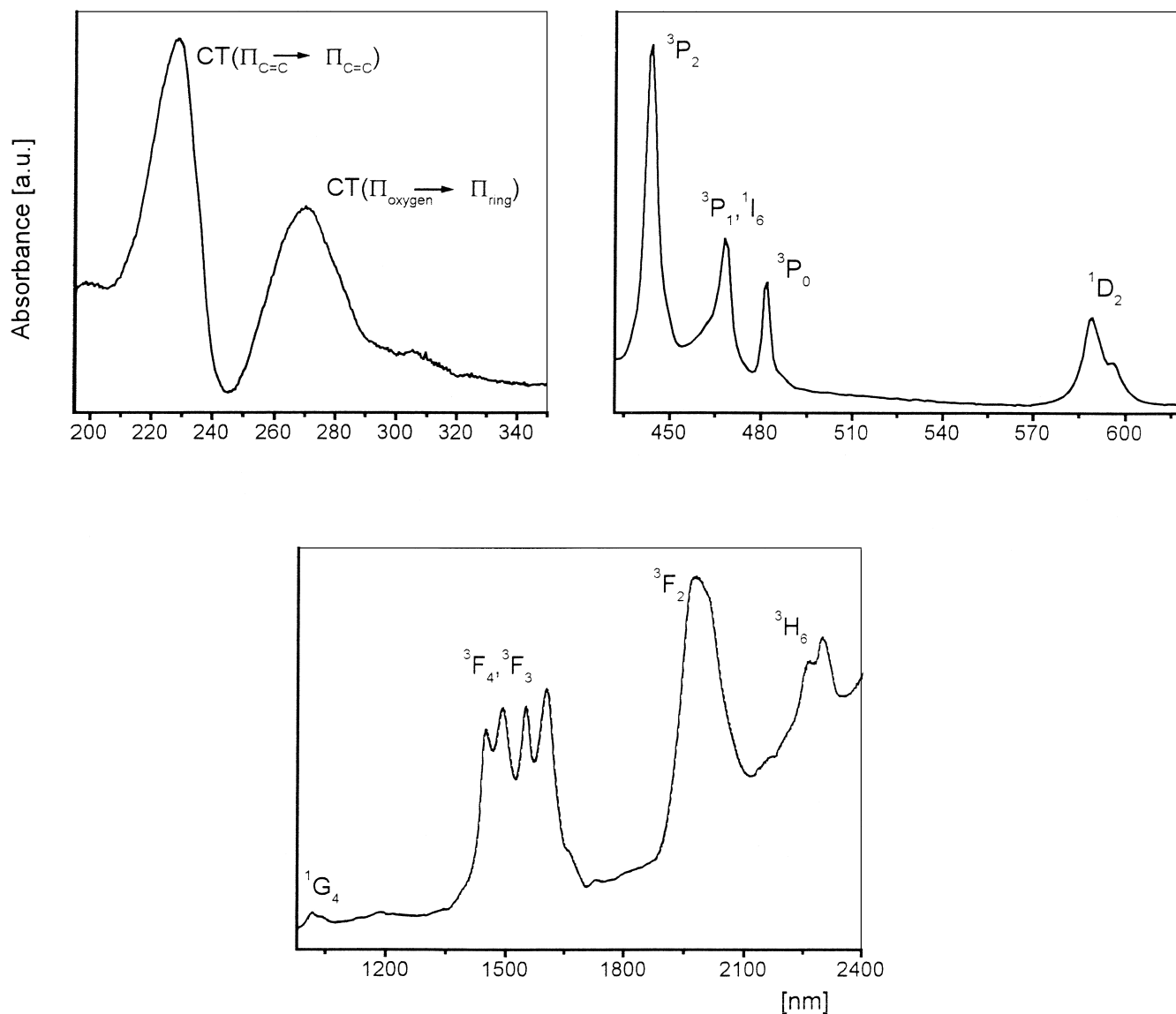
Fig. 2. Room temperature electronic absorption spectrum of the complex (the transitions are from the $^3H_4$ ground state to the [SL]J states).

NIR region, large intensity bands are observed and correspond to the following levels: $^3F_4$ (6897, 6707 cm^{-1}), $^3F_3$ (6452, 6242 cm^{-1}), $^3F_2$ (5056 cm^{-1}) and $^3H_6$ (4415, 4354 cm^{-1}). Almost all bands observed exhibit complex shapes — probably due to more than one site of Pr^{3+} in the complex studied.

In the UV region the complex exhibits two strong and broad bands. The band centered at 230 nm (43,478 cm^{-1}) should be assigned to the excitation of an electron from a skeleton carbon–carbon double bond to a level with a uniform charge distribution over the ligand [13]. The second band at 260 nm (38,462 cm^{-1}) corresponds to the charge transfer $\pi_{oxygen} \rightarrow \pi_{ring}$ transition [14]. These transitions are observed in the spectra of the free ligand at 230 and 275 nm [15], respectively.

3.3. Emission and excitation spectra

The emission and excitation spectra of the complex studied were measured at room and liquid nitrogen temperatures. They are presented in Figs. 3 and 4. The 308 nm excitation line was used in the luminescence measurements and a few emission lines were applied in the excitation experiment (540, 590 and 645 nm).

The excitation within the absorption band, belonging primarily to the ligand transitions (300–400 nm), causes emission from the $^3P_0$ excited state of Pr(III) to the $^3H_4$, $^3H_5$ and $^3H_6$ levels.

The excitation spectra consist of bands corresponding to the $^3P_2$, $^1I_6 + ^3P_1$, $^3P_0$ and $^1D_2$ levels. They appear at 22,989, 21,368, 20,492 and 16,949 cm^{-1}.

The lifetimes of the $^3P_0$ and $^1D_2$ states were determined at 298 K by monitoring the 546 line of the $^3P_0 \rightarrow ^3H_5$ emission and the 587 line of the $^1D_2 \rightarrow ^3H_4$ emission. The excitation used was the 308 nm line of an excimer laser. The values of the lifetimes obtained were $\tau_1 = 150$ ns and $\tau_2 = 615$ ns for the former and $\tau_1 = 110$ ns and $\tau_2 = 555$ ns for the latter transition. These data can be explained as a result of the existence of two structurally different sites for Pr^{3+} in the crystal structure of the complex. This conclusion, however, should be confirmed by further studies, mainly by X-ray structural data. The luminescence and excitation spectra (Figs. 3 and 4) exhibit broad and unsplit bands, which suggests an amorphous structure for part of the sample rather than the existence of two sites of Pr^{3+}. Smaller values of the decay times obtained for the $^1D_2$ level demonstrate stronger quenching of this transition by coupling with the OH vibrations of the coordinated and lattice water molecules. The excitation in these measurements was chosen in the range where ligand absorption occurs. The results obtained show that the ligand triplet levels are in resonance with the excited states of the praseodymium ion.

4. Conclusions

The present studies concern the synthesis, chemical characterisation and spectroscopic data for new six-coordinate praseodymium(III) compounds with 3-halo-2,6-lutidine. The synthesis method described in this paper will be used in the synthesis of the other lanthanide complexes
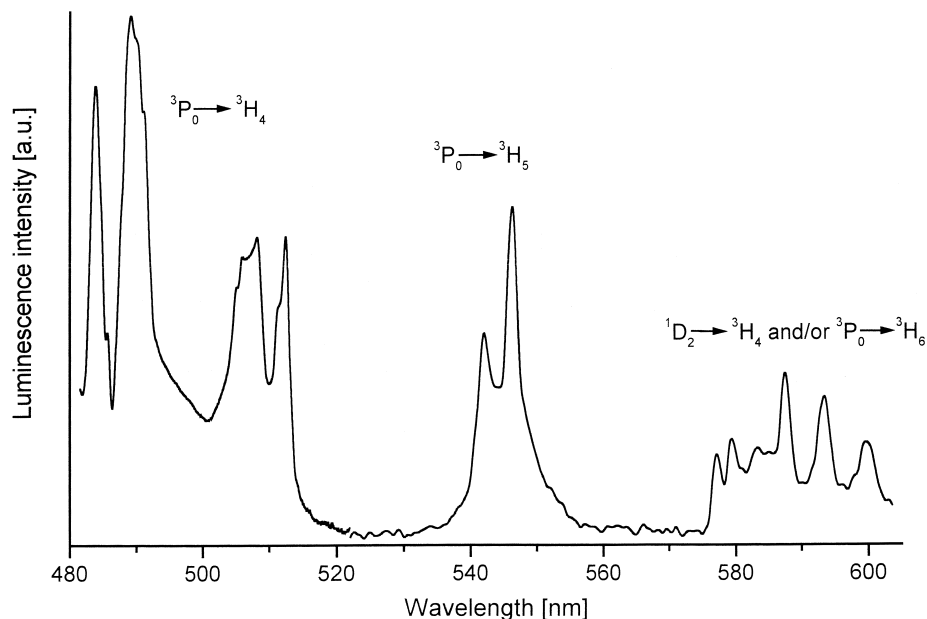

Fig. 3. Emission spectra of the complex measured at room temperature using the $\lambda_{exc} = 308$ nm line.
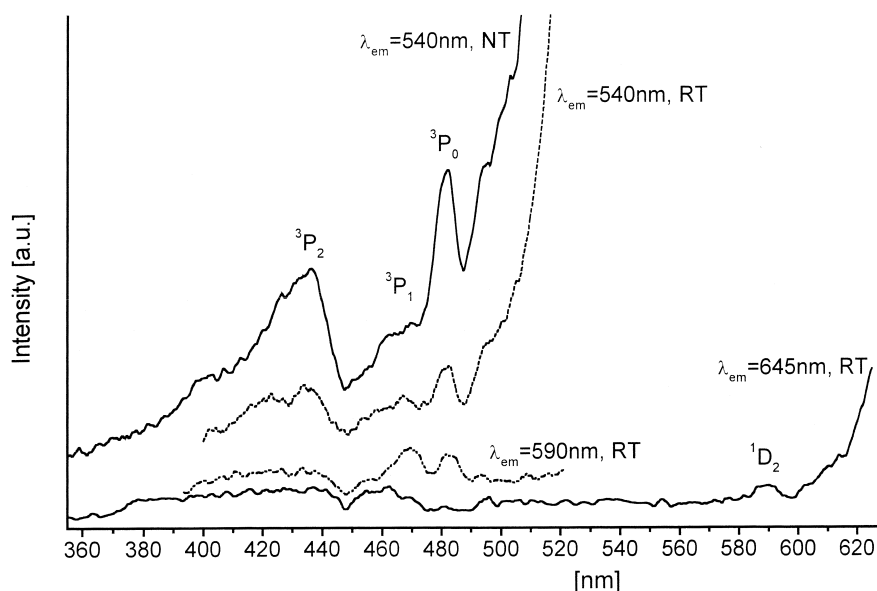
Fig. 4. Excitation spectra of the complex measured at room temperature (λ_{em} = 540, 590 and 645 nm) and liquid nitrogen temperature (λ_{em} = 540 nm).

with a Ln:ligand ratio of 1:3, 1:6, 1:7 and 1:8. The spectroscopic data for these compounds will be compared with those for lanthanum derivatives which will be helpful for interpretation of the spectra. In the present work the following spectroscopic characteristics were obtained:

1. The IR and Raman spectra exhibit a complexation shift of the ν(N–O) band of $\Delta\nu \cong 44$ and 8 cm^{-1}, respectively. The stretching and bending praseodymium oxygen vibrations appear in the ranges 200–300 and 100–150 cm^{-1}, respectively.
2. The electronic absorption spectra exhibit the standard energy sequence characteristic for Pr^{3+}. It contains the $^3P_{0-2}$, $^1I_6$, $^1D_2$, $^1G_4$, $^3F_{2-4}$ and $^3H_6$ multiplets as well as two intra-ligand bands due to CT transitions.
3. Under excitation in the $^3P_0$ state and ligand CT transition, the compound shows emission from the $^3P_0$ and probably from the $^1D_2$ levels.
4. Two exponential decay curves were obtained for the lifetimes of the $^3P_0$ and $^1D_2$ states at RT. These results can be explained as being due to the existence of two kinds of Pr^{3+} centers in the compound. However, this conclusion should be verified in future studies on a single crystal sample.

References

[1] R.G. Garvey, J.H. Nelson, R.O. Ragsdale, Coord. Chem. Rev. 3 (1968) 375.
[2] R.L. Carlin, L.J. deJongh, Chem. Rev. 86 (1986) 659.
[3] J.V. Quagliano, J. Fujita, G. Franz, D.J. Phillips, J.A. Walmsley, S.Y. Tyree, J. Am. Chem. Soc. 83 (1961) 3770.
[4] S. Kida, J.V. Quagliano, J.A. Walmsley, S.Y. Tyree, Spectrochim. Acta 19 (1963) 189.
[5] Y. Kakiuti, S. Kida, J.V. Quagliano, Spectrochim. Acta 19 (1963) 201.
[6] L.R. Melby, N.J. Rose, E. Abramson, J.C. Caris, J. Am. Chem. Soc. 86 (1964) 5117.
[7] V.N. Krishnamurthy, S. Soundararajan, Can. J. Chem. 45 (1967) 189.
[8] A. Razzak, X. Al-Karaghouli, J.S Wood, Inorg. Chem. 18 (1979) 1177.
[9] J. Hanuza, M. Mączka, A. Waśkowska, W. Oganowski, H. Ban-Oganowska, E.T.G. Lutz, J.H. van der Maas, Vibr. Spectrosc. 14 (1997) 49.
[10] J. Hanuza, M. Mączka, A. Waśkowska, W. Oganowski, H. Ban-Oganowska, E.T.G. Lutz, J.H. van der Maas, J. Mol. Struct. 408/409 (1997) 349.
[11] J. Hanuza, M. Mączka, A. Waśkowska, W. Oganowski, H. Ban-Oganowska, E.T.G. Lutz, J.H. van der Maas, J. Chem. Soc., Perkin Trans. 2 (1997) 2039.
[12] J. Hanuza, M. Mączka, A. Waśkowska, W. Oganowski, H. Ban-Oganowska, E.T.G. Lutz, J.H. van der Maas, J. Mol. Struct. 450 (1998) 201.
[13] T. Kubota, Bull. Chem. Soc. Jpn. 35 (1962) 946.
[14] E. Evleth, Theor. Chim. Acta 11 (1968) 145.
[15] H. Ban-Oganowska, Pol. J. Chem. 70 (1996) 1533.